Journal of Applied Polymer Science

Enhanced electrosorption capacity for lead ion removal with polypyrrole and air-plasma activated carbon nanotube composite electrode

Lingfang Yang, Zhou Shi
Department of Water Engineering and Science, College of Civil Engineering, Hunan University, Changsha, Hunan 410082, People's Republic of China
Correspondence to: Z. Shi (E-mail: zhous61@163.com)

ABSTRACT: Polypyrrole (PPy) and air-plasma activated carbon nanotube (CNT) composites (P-CNT-PPy) prepared via *in situ* chemical oxidative polymerization are studied to improve the electrosorption capacity of CNT-based electrodes for the removal of lead ions. For comparison, the PPy prepared on the CNTs without plasma activation is labeled as CNT/PPy. The morphology of the composite was observed by scanning electron microscopy (SEM), and pore structures were studied by N_2 adsorption-desorption isotherms. The electrochemical capacitance properties of the composite were measured by cyclic voltammetry (CV), electrochemical impedance spectroscopy (EIS), and galvanostatic charge-discharge in lead solutions. With plasma-activation, the specific surface area of the P-CNT-PPy composite is larger than that of CNT/PPy. Additionally, the P-CNT-PPy composites exhibit excellent electrochemical performance in lead solution, with a higher specific capacitance and smaller charge transfer resistance than that of CNT/PPy. XPS elemental analysis and electrosorption and regeneration results show that the electrosorption and desorption process is reversible under a voltage of 450 mV. The electrosorption kinetics of P-CNT-PPy electrodes abide by pseudo-second-order model reaction. The lead ion electrosorption experiments agree with the Langmuir model, and the equilibrium electrosorption capacity of the P-CNT-PPy electrodes is 3.6 and 1.3 times higher than that of the CNT and CNT/PPy, respectively. © 2014 Wiley Periodicals, Inc. J. Appl. Polym. Sci. **2015**, *132*, 41793.

KEYWORDS: adsorption; composites; conducting polymers

Received 7 September 2014; accepted 22 November 2014
DOI: 10.1002/app.41793

INTRODUCTION

The lead ion (Pb^{2+}) is a common hazardous pollutant in wastewater and generally discharged by metal plating facilities, mining operations, fertilizers, batteries, and pesticide industries, etc. Once lead accumulates in the human body, it can cause severe damage to the kidney, nervous system, reproductive system, liver, and brain.[1] High concentrations of lead in wastewater can be easily treated by various methods, such as chemical precipitation,[2] ion exchange,[3] adsorption,[4] and electrochemical treatment technologies.[5] However, these treatments become difficult and costly when the lead ion concentration is low. In previous studies, we have found that capacitive deionization (CDI) is a promising technique to remove lead ions from aqueous solutions, because of its advantages of energy efficiency and simple regeneration.[6] When a pair of parallel electrodes are charged in aqueous solutions, ions will move toward the counter electrode to form electric double layer between the water and the electrode interface, thus removing ions from water.[7] When the applied voltage is set to zero, the adsorbed ions are released back to solution, realizing the electrodes' regeneration.

Ion electrosorption capacity is an important consideration when selecting electrode materials. Conventional electrode materials are carbon-based materials such as activated carbon,[8] activated carbon cloth,[9] carbon aerogels,[10] carbide-derived carbons,[11] carbon nanotubes (CNTs),[12] and graphene.[13] Generally, a capacitor prepared from carbon-based materials is classified as an electric double-layer capacitor, whose electrosorption only occurs at the interface between the electrode and solution. The electrosorption capacity mainly depends on the effective specific surface area (SSA) of the electrode. Therefore, the specific capacitance of CNTs is relative small due to low utilization of the SSA. Pseudo-capacitors, which are made from conducting polymers and their composites, have specific capacitances much higher than those of the electric double layer capacitors.[14] Conducting polymers such as polyaniline and polypyrrole are promising electrode materials due to their good electrical conductivity,

large capacitance, and low cost.[15,16] Polypyrrole (PPy) is one of the most studied conducting polymer materials because of its environmental stability and easy synthesis. Although PPy shows advantages in electrosorption applications, it suffers from relatively lower conductivity, smaller specific surface area and smaller pore volumes than carbon materials. When used as electrosorption electrodes, the continuous swelling/shrinkage of the interlaced PPy chains that occurs during the charge/discharge processes typically results in inadequate release of ionic carriers, thus leading to poor cyclic stability. Researchers have attempted to solve these problems by combining CNTs with PPy, based on the synergistic effects to improve the performance of both the CNTs and the PPy. These composites were mostly used as electrode materials for energy storage applications.[17,18] There are few studies on the applications of carbon and PPy composites in CDI. Recently, Zhang *et al.*[19] and Liu *et al.*[20] used PPy and graphite composites as electrode materials for CDI process.

In this article, two kinds of CNT and PPy composites are prepared for the electrosorption of lead ions. The first, labeled CNT/PPy, is directly prepared with CNT via *in situ* chemical oxidative polymerization. This kind of composite improved the electrosorption performance over single phase CNTs. However, since the solubility of the CNTs is poor, the PPy has poor dispersibility across the CNT surface, and the synergistic effects between two materials remain negligible due to self-polymerization that occurs in part of the PPy. Moreover, there is little interaction between CNT and PPy, resulting in low charge-transfer and high interfacial resistance between the CNT and PPy. To overcome these disadvantages, a second composite, labeled P-CNT-PPy, is studied. In the synthesis of this composite, a solvent-free approach is presented to functionalize the CNTs with oxygen- and nitrogen-containing surface groups via air-plasma activation to improve the poor solubility of CNTs as shown in previous work.[6] The plasma activation process also provides a hydrophilic surface onto which it is possible to graft PPy without damaging the CNT structure, which represents a marked improvement over conventional strong acid treatments.[21–23] Moreover, air-plasma activation introduces nitrogen-containing groups. According to Haq *et al.*,[24] the N-doping sites on the CNT backbone provide active nucleation sites for the covalent bonding with conducting polymers. In the following sections, the electrochemical properties and electrosorption characteristics of the CNT/PPy and P-CNT-PPy composite electrodes are studied and compared in lead solution.

EXPERIMENTAL

Preparation of Plasma Activated CNTs

The CNTs used in the study were purchased from Shenzhen Nanotech Port, China. Specifications of the CNTs are as follows: length <2 μm, diameter 20–40 nm, surface area 130–160 m^2/g, purity $>97\%$, and ash content $<3\%$.

Air-plasma was excited by radio-frequency (RF) inductively coupled plasma (ICP). The plasma treatment was carried out in a horizontally installed cylindrical reactor of quartz glass with dimensions of 30 mm (outer diameter) $\times$ 100 mm (length).[25] The CNTs are homogeneously and thinly placed on the cylinder wall. The spiral coil was fixed outside the reactor. Prior to ignition, the reactor was evacuated to 10 Pa. Then air flowed into the reactor via a needle valve to maintain a constant pressure. The plasma was ignited at 10 Pa, and the RF amplifier was set to 130 mA, 650 V with frequency of 13.56 MHz. The CNTs were activated by air plasma for 20 min.

Preparation of P-CNT-PPy Composites and Electrodes

Plasma-activated CNTs (250 mg) were added to a 300 mL aqueous solution containing 0.5 g of ammonium peroxydisulfate (APS) and 10 mL of HCl (12 mol/L). One milliliter of pyrrole monomer (purity 98%) was added to this solution and stirred for 30 min. A further 2 g of APS was then dissolved in a 50 mL aqueous solution, which was added to the mixture above. The mixture was maintained at 0–4°C for 8 h, with continuous mechanical stirring. The composite was collected using filtration and repetitive washing with pure water and ethanol until the water was colorless, and was then dried for 24 h at 60°C. The composite was named as P-CNT-PPy. For comparison, the CNT/PPy composite was prepared using the same proportions on the CNTs without plasma activation.

The composites were then mixed with carbon black and polytetrafluoroethylene (PTFE) at a weight ratio of 80 : 10 : 10 in a few drops of ethanol. To make electrodes, the mixture (50 mg) was coated onto current collector (nets made of stainless steel wire with a shape of 30 $\times$ 50 mm^2), and the collector was pressed by a hydraulic cylinder at 10 MPa for 10 min; it was then dried in an oven for 24 h at 120°C. For the electrochemical test, the mass of active material was about 2 mg on a current collector with the area of 1 cm^2.

Composite and Electrode Characterization

Surface area and pore size distribution were analyzed from N_2 adsorption-desorption isotherms obtained at 77 K using a adsorption apparatus (Quantachrome NOVA4000, USA). The surface morphologies were obtained by a scanning electron microscope (SEM, Hitachi S-4800, Japan). Electrochemical properties were measured by cyclic voltametry (CV), electrochemical impedance spectroscopy (EIS), and galvanostatic charge-discharge in a typical three electrodes cell at 20°C with a potentiostat analyzer (CHI660E, CH Instrument, China). In the CV process, platinum foil, a calomel electrode and a 50 mg/L lead ion solution (prepared with $Pb(NO_3)_2$) were used as the counter, reference electrode, and electrolyte, respectively.

Electrosorption Capacity Measurement

To investigate the electrosorption capacity of the composite electrodes, a bench scale experimental setup was adopted. This system consists of four planar capacitor units and a power supply. The lead solution (200 mL, pH 6) was circulated in the capacitors and feed tank by a peristaltic pump. The solution was kept at temperature of 20°C. The flow rate and supply voltage were set to 20 mL/min and 450 mV, respectively. The distance between the electrodes was 3 mm and the area of working electrode was 60 cm^2. The Pb ion concentration was measured by an atomic absorption spectrophotometer (Shimadzu AA-7000). The electrosorption capacity (q_e, mg/g) of the electrodes was calculated using eq. (1):

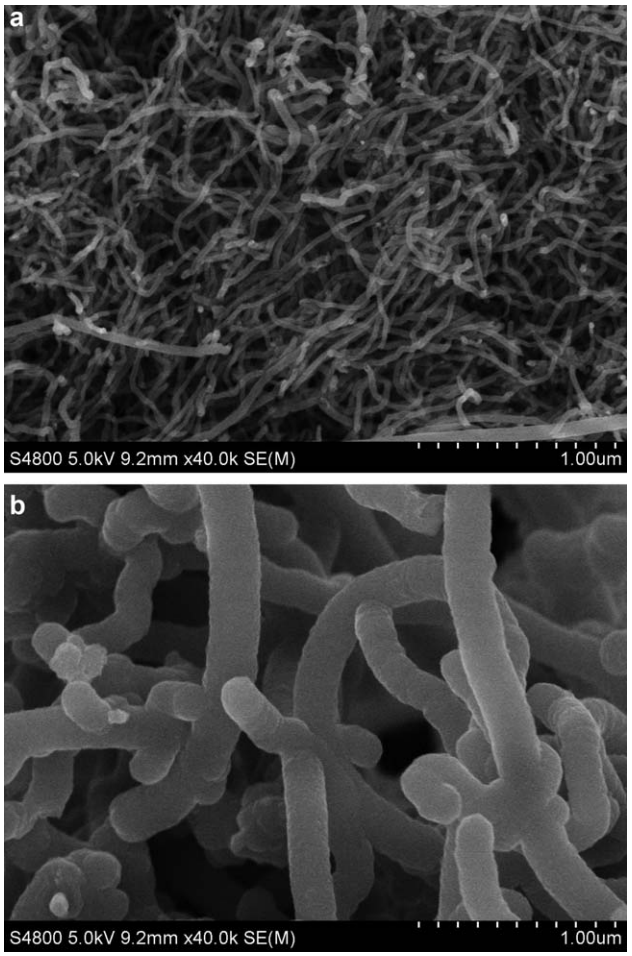

Figure 1. SEM images of (a) plasma activated CNT and (b) P-CNT-PPy.

$$q_e = \frac{(c_0 - c_t)V}{m} \quad (1)$$

where c_0 (mg/L) and c_t (mg/L) are the initial and final lead ions concentrations, respectively, V (mL) is the lead solution volume, and m (g) is the mass of activate materials in the working electrodes.

RESULTS AND DISCUSSION

Materials Characterization

The surface morphologies of the plasma activated CNT and P-CNT-PPy composites were examined with SEM, as seen in Figure 1. In Figure 1(a), the plasma activated CNTs show typical CNT morphology and there is no obvious damage to the structure of the CNTs. In Figure 1(b), PPy is tightly and uniformly coated onto the nanotube, and parts of the nanotubes are joined by the PPy.

Figure 2 shows the nitrogen adsorption/desorption isotherms and BJH pore size distribution of the CNTs, CNT/PPy, and P-CNT-PPy composites. As shown in Figure 2(a), a hysteresis loop in the adsorption/desorption isotherm shows the type IV pattern as defined by IUPAC, which is characteristic of mesoporous structure. From Figure 2(a), it is clear that the P-CNT-PPy has a higher nitrogen adsorption capacity than that of CNT/PPy. The BET surface area of the CNTs, CNT/PPy, and P-CNT-PPy composites are 280, 42, and 80 m^2/g, respectively. Clearly, the specific surface area of the composite can be improved by grafting the PPy to the CNTs (SSA of pure PPy: 18 m^2/g), and further enhanced when grafted to air-plasma activated CNTs. Because of the existence of oxygen- and nitrogen-containing groups on the surface of plasma activated CNTs,[6] the CNTs disperse well in water solution and provide the pyrrole with more activated sites to grow and wrap up. As shown in the pore size distribution, the P-CNT-PPy composite has a larger pore volume than the CNT/PPy: the peak diameter is 2 nm for CNT/PPy, and 2–4 nm for P-CNT-PPy. As discussed in our previous work,[6] the lead ions can diffuse more freely with the increase of mesoporous volume.

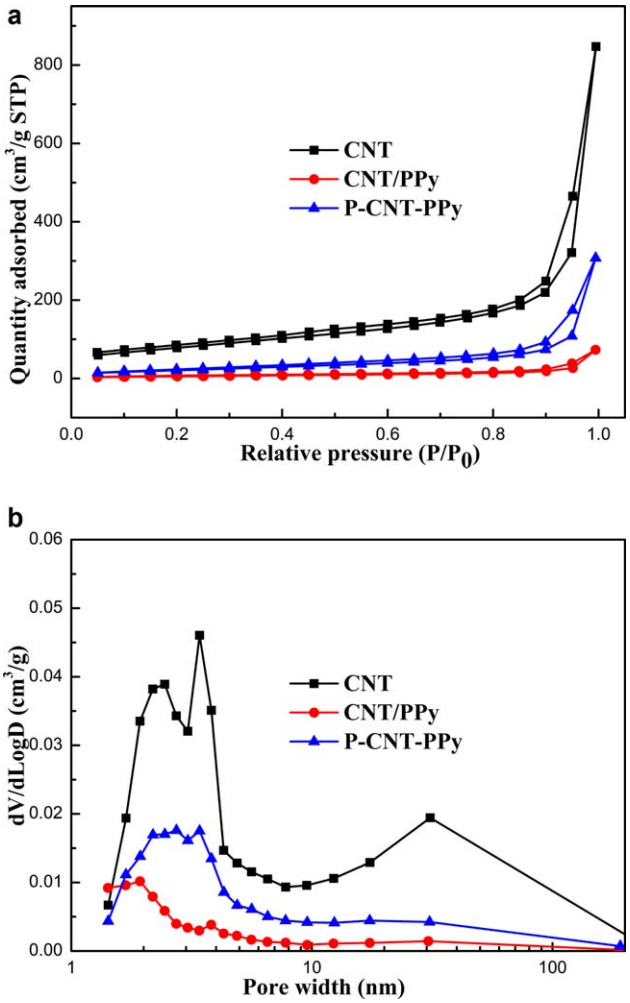

Figure 2. Nitrogen adsorption/desorption isotherms (a) and BJH pore size distributions for the CNTs, CNT/PPy, and P-CNT-PPy composites. [Color figure can be viewed in the online issue, which is available at wileyonlinelibrary.com.]

Figure 3(a) shows the cyclic voltammetry (CV) results of the CNT, CNT/PPy, and P-CNT-PPy composite electrodes at scan rate of 10 mV/s within the potential window of −0.5 to 0.2 V. The area enveloped by the curves represents the capacitance of the electrode. Obviously, the P-CNT-PPy electrode has the

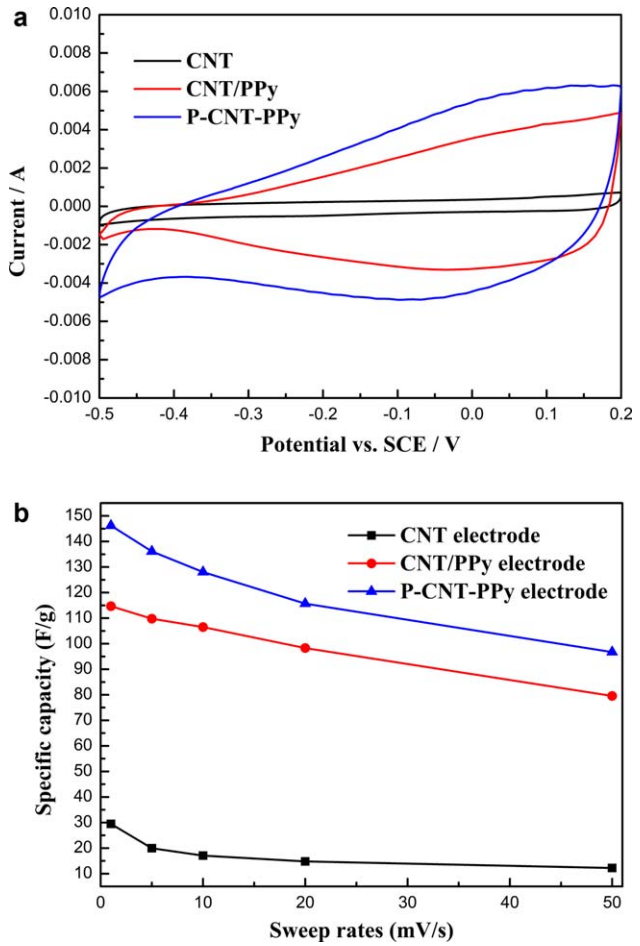

Figure 3. Cyclic voltammetry at the scan rate of 10 mV/s (a) and specific capacitance at different sweep rates (b) in 50 mg/L lead aqueous solutions. [Color figure can be viewed in the online issue, which is available at wileyonlinelibrary.com.]

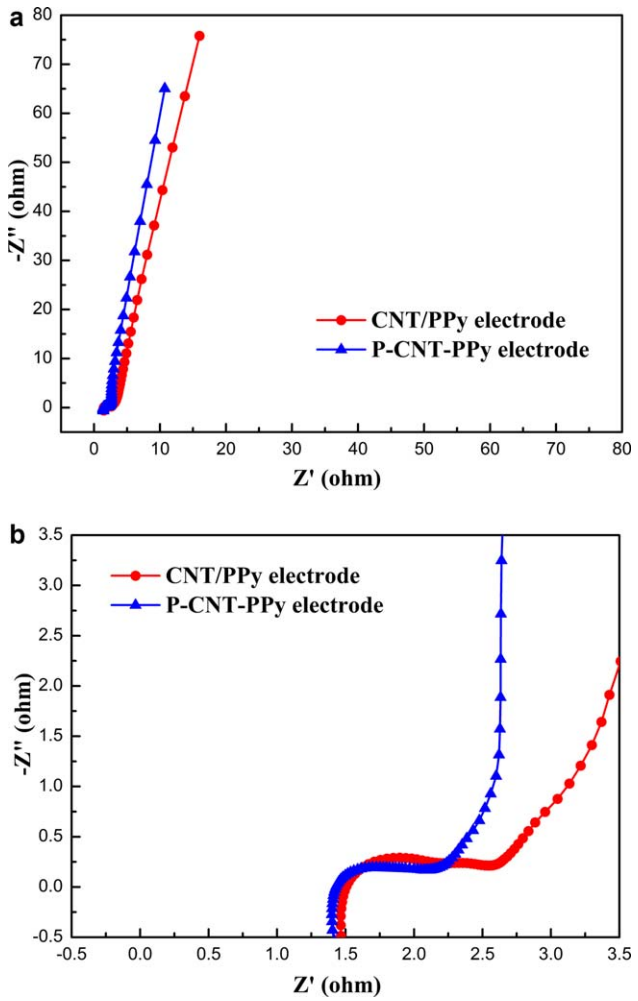

Figure 4. Impedance Nyquist plots measured in 50 mg/L lead aqueous solutions (a) and details of high-frequency region (b). [Color figure can be viewed in the online issue, which is available at wileyonlinelibrary.com.]

largest area and the highest specific capacitance. The specific capacitance can be calculated from the CV curve using eq. (2):

$$C = \frac{\int_{E_1}^{E_2} idE}{v(E_2 - E_1)m} \quad (2)$$

where i is the scan current (A), E_1 and E_2 are the low-limit and upper-limit potential (V), respectively, v is the scan rate (V/s), and m is the active material mass (g). The specific capacitances at different sweep rates are shown in Figure 3(b). The specific capacitances of P-CNT-PPy, CNT/PPy, and CNT electrode, are 128, 108, and 17 F/g, respectively. The specific capacitance of CNT/PPy electrode is 5.3 times larger than that of CNT electrode with the introduction of the conducting polymer PPy. The specific capacitance and response current of the composite electrodes are further improved by air-plasma treatment. The possible reasons are following: first, the specific surface area of P-CNT-PPy is larger than CNT/PPy; second, the interaction between the CNTs and the PPy is enhanced by the oxygen- and nitrogen-containing groups on the plasma-activated CNTs surface.

The electrochemical impedance spectroscopy (EIS) for P-CNT-PPy and CNT/PPy electrodes is shown in Figure 4. The difference of the real part of impedance between low and high frequencies [which is calculated from Figure 4(b) by taking the diameter of the semicircle] is used to evaluate the electrochemical charge transfer resistance (R_{ct}), which constitutes the main resistance of supercapacitors.[26] The R_{ct} of the P-CNT-PPy electrode is smaller than that of CNT/PPy electrode. The results of the EIS experiments further prove that the P-CNT-PPy composites possess the properties for quick electron transport and charge transfer at the electrode/solution interface. This is due to the oxygen-containing and nitrogen-containing groups on the surface of the CNTs, which produce stronger interactions between the CNTs and the PPy, resulting in smaller R_{ct} resistances.

From the above CV and EIS results, the capacity and conductivity of the P-CNT-PPy composites are improved. As discussed above, the hydrophilic surface of the plasma activated CNTs provides more opportunities for PPy combination, resulting in high specific surface area. Moreover, the N- containing and O-containing groups on the surface of the plasma activated CNTs enhance the interaction between the CNTs and the PPy; this interaction can also strengthen the conductivity and electron

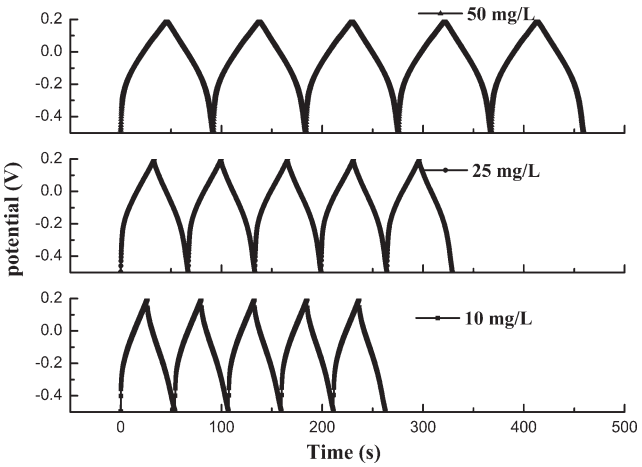

Figure 5. Galvanostatic charge/discharge curves of P-CNT-PPy composite electrode with current density of 5 mA/cm^2 at different lead concentrations.

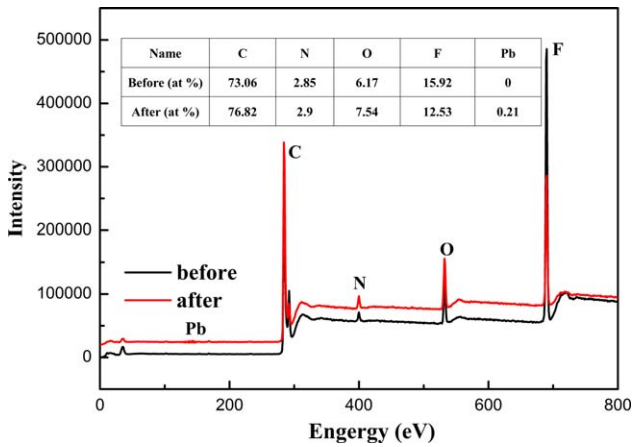

Figure 7. Comparison of XPS analysis of P-CNT-PPy electrode before and after electrosorption and desorption circulation. [Color figure can be viewed in the online issue, which is available at wileyonlinelibrary.com.]

delocalization, which therefore increases the rapid charging/discharging abilities and specific capacitance.

Since the electrodes used in CDI process follows the same concept of electric charge separation as a capacitor. Galvanostatic charge–discharge measurements were conducted to characterize the electrochemical performance related to electrosorption process. Figure 5 shows the galvanostatic charge/discharge curves of P-CNT-PPy electrode with a current density of 5 mA/cm^2, and different lead concentrations. As shown in Figure 5, all curves exhibit an approximately triangular shape, indicative of linear voltage-time dependence. The symmetric charge/discharge characteristics demonstrate typical capacitive behavior, which is associated with good reversibility in this voltage window. Additionally, the specific capacitance increases with lead concentration.

Electrosorption Characterizations

The ion removal performance of the CNT/PPy and P-CNT-PPy electrodes are investigated using lead solution of 10 mg/L under the voltage of 450 mV, and results are shown in Figure 6. The electrosorption capacity of lead ions is determined by eq. (1), and the results are 3.85 and 4.28 mg/g for CNT/PPy and P-CNT-PPy, respectively. As previously mentioned, the surface area and specific capacitance are regarded as the most important factors of electrodes for ion sorption. Materials with high SSA and specific capacitance usually show high ion sorption capacity. The regeneration was conducted by shorting the circuit and the results are shown in the second half of Figure 6 (after 40 min). After removing the voltage, the electrosorbed lead ions are almost all released. This proves that the lead was not oxidized or reduced during the electrosorption process under this voltage. From the CV test shown in Figure 3(a), typical capacitor-like characteristics can also be observed. There were no evident redox reactions occurring in the applied potential range of −0.5 to 0 V.

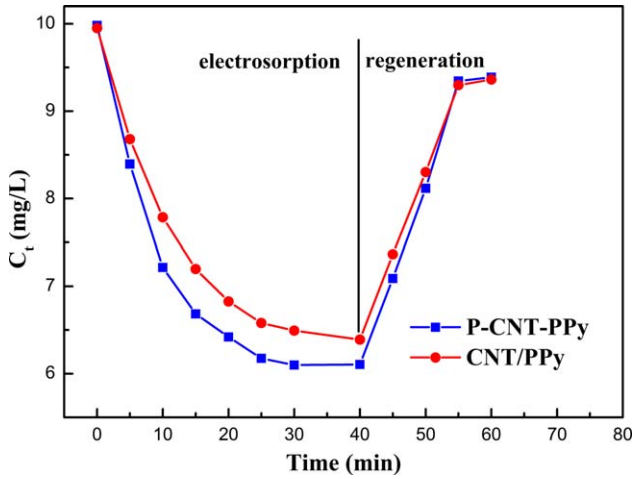

Figure 6. Lead ions electrosorption and regeneration results of P-CNT-PPy and CNT/PPy electrodes under 450 mV. [Color figure can be viewed in the online issue, which is available at wileyonlinelibrary.com.]

To further verify whether the lead ions are oxidized or reduced on the surface of electrode after a long electrosorption and desorption time, the surface element composition of P-CNT-PPy electrode after four cycles, was analyzed by XPS spectra (Figure 7). Before the XPS measurement, the electrode was washed with deionized water to remove most of the residual lead ions. It can be observed that the atomic ratio of lead is only 0.21%. This provides further confirmation that lead ions are not removed by electrochemical reaction. Therefore, it is determined that the electrosorption and desorption process is reversible under the voltage of 450 mV.

The pseudo-first-order and pseudo-second-order kinetic models are employed to fit the experimental data. The linear forms of these two models are described as follows:

$$\ln(q_e - q_t) = \ln q_e - k_1 t \quad (3)$$

$$\frac{t}{q_t} = \frac{1}{k_2 q_e^2} + \frac{1}{q_e} t \quad (4)$$

where k_1 and k_2 is the adsorption rate constant, q_e and q_t is the amounts of lead electrosorbed at equilibrium and time t, respectively. The electrosorption fitting parameters and correlation coefficients of the pseudo-first-order and pseudo-second-

Table I. Electrosorption Parameters of Pseudo-First-Order and Pseudo-Second-Order Kinetics for Lead Ions

	Pseudo-first-order			Pseudo-second-order		
Electrodes	q_e	k_1 ($\times 10^{-2}$)	R^2	q_e	k_2 ($\times 10^{-2}$)	R^2
CNT/PPy	3.99	11.4	0.9876	5.00	1.8	0.9919
P-CNT-PPy	4.50	13.3	0.9916	5.56	2.2	0.9956

order kinetic models determined by eqs. (3) and (4) are listed in Table I, and their fitting curves are shown in Figure 8. It can be seen that the pseudo-second-order kinetic model fits the experimental results better than the pseudo-first-order kinetic model for the higher value of correlation coefficients. The electrosorption rate constant indicates the removal rate of lead ions. From Table I, the electrosorption rate constant of P-CNT-PPy is larger than that of CNT/PPy in both kinetic models. The removal rate may depend on the electrochemical properties and the pore structure. As discussed in the EIS results, the P-CNT–PPy shows better electrical conductivity than the CNT/PPy due to small R_{ct}. Enhanced electrical conductivity accelerates the charging process and movement of lead ions in the PPy skeleton as described in following eq. (6). In addition, the increased mesoporous volume facilitates fast entrance of ions into electrode.

The electrosorption isotherms of the CNT, CNT/PPy, and P-CNT-PPy electrodes, as well as the fitting lines by Langmuir model, are shown in Figure 9. The initial concentrations of lead solutions are 5, 10, 20, 30, and 50 mg/L, respectively. The electrosorption capacity is improved with the increase of initial concentration as discussed in the section "Materials Characterization" galvanostatic charge/discharge tests. The data is fitted by the Langmuir isotherm, as given by eq. (5):

$$q = \frac{q_m K_L C}{1 + K_L C} \tag{5}$$

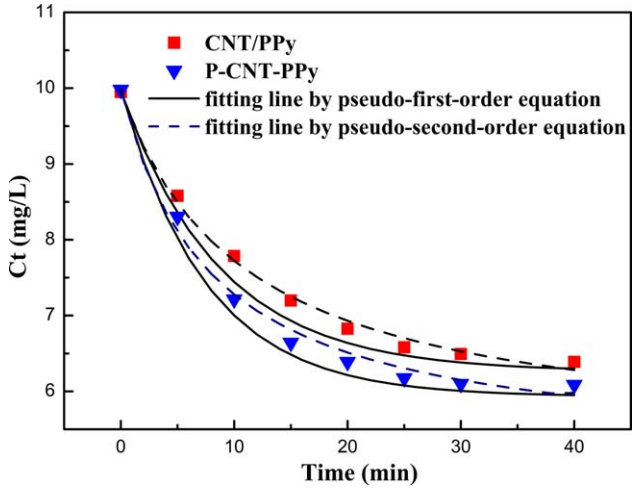

Figure 8. Pseudo-first-order and pseudo-second-order kinetic of lead ions removal. [Color figure can be viewed in the online issue, which is available at wileyonlinelibrary.com.]

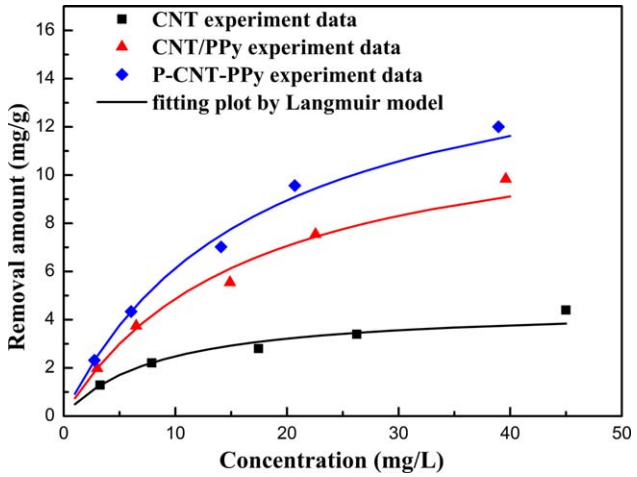

Figure 9. Electrosorption isotherm of CNT, CNT/PPy, and P-CNT-PPy electrodes and the fitting plot by Langmuir model. [Color figure can be viewed in the online issue, which is available at wileyonlinelibrary.com.]

where C is the lead concentration (mg/L), q is the amount of lead adsorbed at equilibrium (mg/g), and q_m is the maximum adsorption capacity corresponding to complete monolayer coverage (mg/g). Table II shows the parameters of Langmuir isotherms. As shown in Figure 9, the experimental results fit well with the Langmuir adsorption model, indicating that electrosorption follows the rule of monolayer adsorption. The equilibrium electrosorption capacity of P-CNT-PPy electrode is 16.55 mg/g, which is nearly 3.6 and 1.3 times than that of CNT and CNT/PPy electrode, respectively. Normally, the electrosorption capacitance of the CNT electrodes, whose electrosorption only occurs at the interface between the electrode and solution, depends mainly on the effective specific surface area of electrodes. As for CNT and PPy composite electrodes, there is not only a double electrical layer existing in the interface between the electrode and solution, but also the charge transfer in PPy skeleton defined by the following equation:

$$\mathrm{PPy} + \mathrm{e} \xrightarrow{\text{charge}} \mathrm{PPy}^- \tag{6}$$

In the electrosorption process, the PPy skeletons of the cathode gain electrons to form negative valence PPy. The positive charges, such as lead ions, gather nearby the negative valence PPy to maintain neutral, thus being electrosorbed. Once the voltage is removed, the equation operates reversely, and the lead ions return to solution. This kind of ion adsorption caused by PPy's Faradic reaction takes place not only on the surface but also in the interior of the electrode, and this part of electrosorption is usually much larger than that caused by electrical double

Table II. Isotherms Parameters of Lead Electrosorption with Different Electrodes

Electrodes	q_m	k_L	R^2
CNT	4.54	0.12	0.9881
CNT/PPy	12.85	0.06	0.9961
P-CNT-PPy	16.55	0.06	0.9984

layer. Therefore, it verifies that the electrosorption capacity of CNT/PPy electrode is greater than that of CNT electrodes.

CONCLUSIONS

PPy and CNT composites are studied to improve the electrosorption capacity of CNT-based electrodes for the removal of lead ions from wastewater. The air-plasma treatment technique is employed to improve the electrosorption properties of the composites. The P-CNT-PPy composites are prepared via in situ chemical oxidative polymerization with plasma-activated CNTs. SEM results show that the PPy is uniformly coated on the surface of the plasma activated CNTs. The P-CNT-PPy presents excellent properties with larger BET surface areas, more mesoporous volumes, higher specific capacitance, smaller R_{ct}, better electrical conductivity and faster charging/discharging rate than the electrode prepared by PPy coating on the CNT without plasma activation (CNT/PPy). CV testing, XPS elements analysis, electrosorption, and regeneration results all show that the electrosorption and desorption process is reversible for the composites under the voltage of 450 mV. The electrosorption kinetics of the CNT/PPy and P-CNT-PPy electrodes abide by the pseudo-second-order model reaction. The lead ion electrosorption experiments agree with the Langmuir model, and the equilibrium electrosorption capacity of P-CNT-PPy is nearly 3.6 and 1.3 times than that of CNT and CNT/PPy electrodes. The P-CNT-PPy composites presented here therefore represent very promising materials for CDI of lead removal.

ACKNOWLEDGMENTS

This work was supported by the National Science & Technology Pillar Program of China, the Twelfth Five-year Plan under contract No. 2012BAJ24B03.

REFERENCES

1. Fu, F.; Wang, Q. *J. Environ. Manage.* **2011**, *92*, 407.
2. Liu, L.; Wu, J.; Li, X.; Ling, Y. *Sep. Purif. Technol.* **2013**, *103*, 92.
3. Priybrata, P.; Fawzi, B. *J. Nat. Gas Sci. Eng.* **2014**, *18*, 227.
4. Lzquierdo, M. T.; de Yuso, A. M.; Valenciano, R.; Rubio, B.; Pino, M. R. *Appl. Surf. Sci.* **2013**, *264*, 335.
5. Souilah, O.; Akretche, D. E.; Cameselle, C. *Electrochim. Acta* **2012**, *86*, 138.
6. Yang, L.; Shi, Z.; Hao, W. *Surf. Coat. Technol.* **2014**, *251*, 122.
7. Porada, S.; Zhao, R.; van der Wal, A.; Presser, V.; Biesheuvel, P. M. *Prog. Mater. Sci.* **2013**, *58*, 1388.
8. Hou, C. H.; Huang, C. Y. *Desalination* **2013**, *314*, 124.
9. Huang, C.; Su, Y. *J. Hazard. Mater.* **2010**, *175*, 477.
10. Rasines, G.; Lavela, P.; Macias, C.; Haro, M.; Ania, C. O.; Tirado, J. L. *J. Electroanal. Chem.* **2012**, *671*, 92.
11. Porada, S.; Weinstein, L.; Dash, R.; van der Wal, A.; Bryjak, M.; Gogotsi, Y.; Biesheuvel, P. M. *Appl. Mater. Interfaces* **2012**, *4*, 1194.
12. Dai, K.; Shi, L.; Fang, J.; Zhang, D.; Yu, B. *Mater. Lett.* **2005**, *59*, 1989.
13. Li, H.; Zou, L.; Pan, L.; Sun, Z. *Sep. Purif. Technol.* **2010**, *75*, 8.
14. Sharma, K.; Rastogi, A. C.; Desu, S. B. *Electrochem. Commun.* **2008**, *10*, 268.
15. Han, J.; Xu, G.; Ding, B.; Pan, J.; Dou, H.; MacFarlane, D. R. *J. Mater. Chem. A* **2014**, *2*, 5352.
16. Arcila-Velez, M. R.; Roberts, M. E. *Chem. Mater.* **2014**, *26*, 1601.
17. Wang, J.; Xu, Y.; Chen, X.; Sun, X. *Compos. Sci. Technol.* **2007**, *67*, 2981.
18. Huo, X.; Zhu, P.; Han, G.; Xiong, J. *Carbon* **2014**, *70*, 319.
19. Zhang, Y.; Wang, Y.; Xu, S.; Wang, J.; Wang, Z.; Wang, S. *Synth. Met.* **2010**, *160*, 1392.
20. Liu, Q.; Wang, Y.; Zhang, Y.; Xu, S.; Wang, J. *Synth. Met.* **2012**, *162*, 655.
21. Hermas, A. A.; Al-Juaid, S. S.; Al-Thabaiti, S. A.; Qusti, A. H.; Salam, M. A. *Prog. Org. Coat.* **2012**, *75*, 404.
22. Sun, X. F.; Xu, Y. L.; Wang, J. *J. Solid State Electrochem.* **2012**, *16*, 1781.
23. Zhang, J.; Kong, L.; Cai, J.; Luo, Y.; Kang, L. *Electrochim. Acta* **2010**, *55*, 8067.
24. Haq, A. U.; Lim, J.; Yun, J. M.; Lee, W. J.; Han, T. H.; Kim, S. O. *Small* **2013**, *9*, 3829.
25. Yang, L.; Shi, Z.; Yang, W. *Water Sci. Technol.* **2014**, *69*, 2272.
26. Tuken, T.; Yazici, B.; Erbil, M. *Prog. Org. Coat.* **2014**, *50*, 115.